

SUPPLEMENTAL DATA

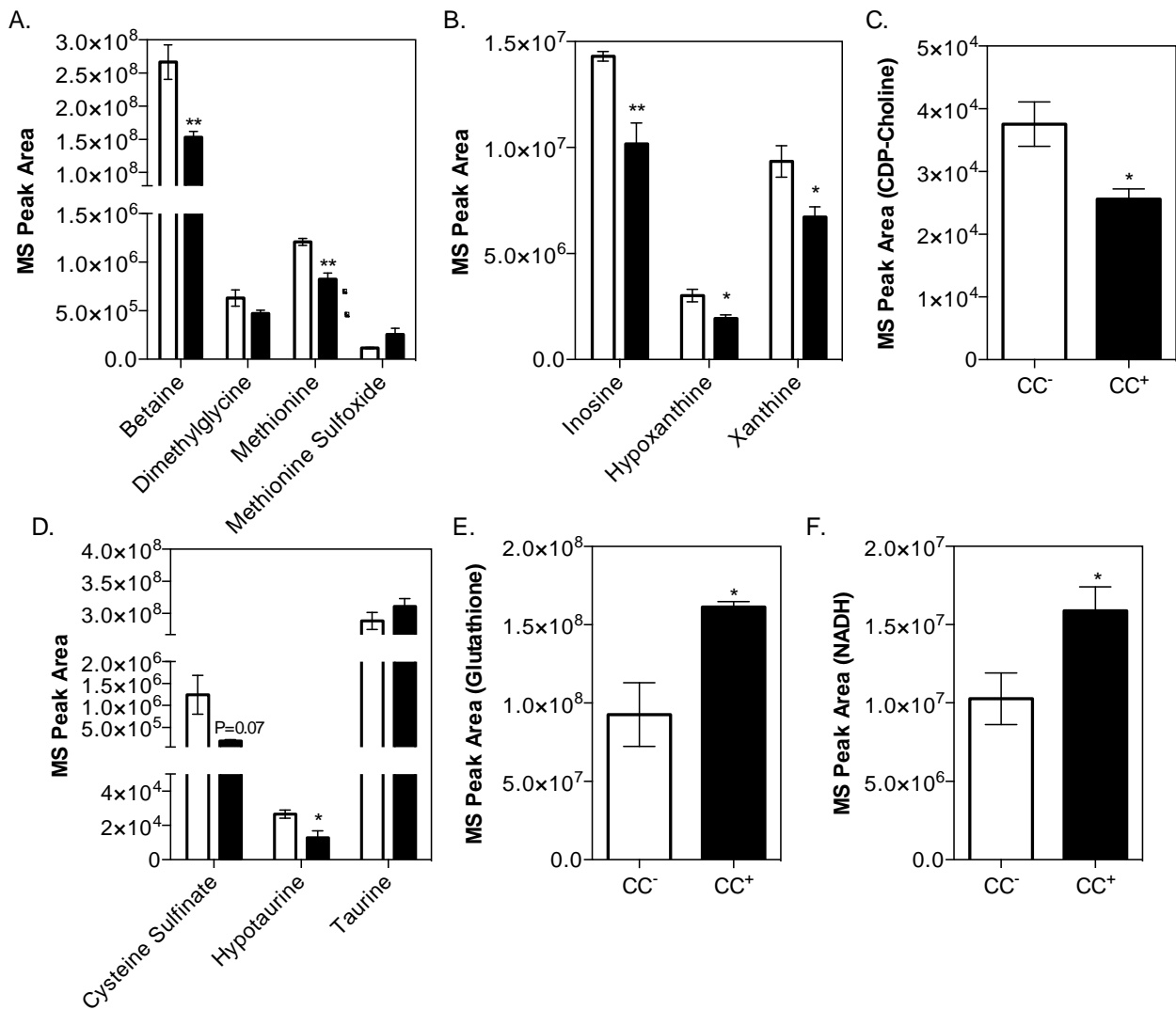


Fig. S1. Analysis of hepatic metabolites involved in one-carbon, transsulfuration, and purine metabolism. Related to Fig. 3 and Table S1. uHPLC-MS/MS analysis of hepatic metabolites from mice colonized with either the CC⁻ (white bars) or CC⁺ (black bars) community maintained on a 1% choline diet for two weeks (5 animals in each experimental group). (A) One-carbon metabolism, (B) Purine metabolism, (C) CDP-choline, (D) Transsulfuration pathway, (E) Glutathione, and (F) NADH. All values are averages ± SEMs. Values that were significantly different (Student's t-test) are indicated: *, P < 0.05; **, P < 0.01.

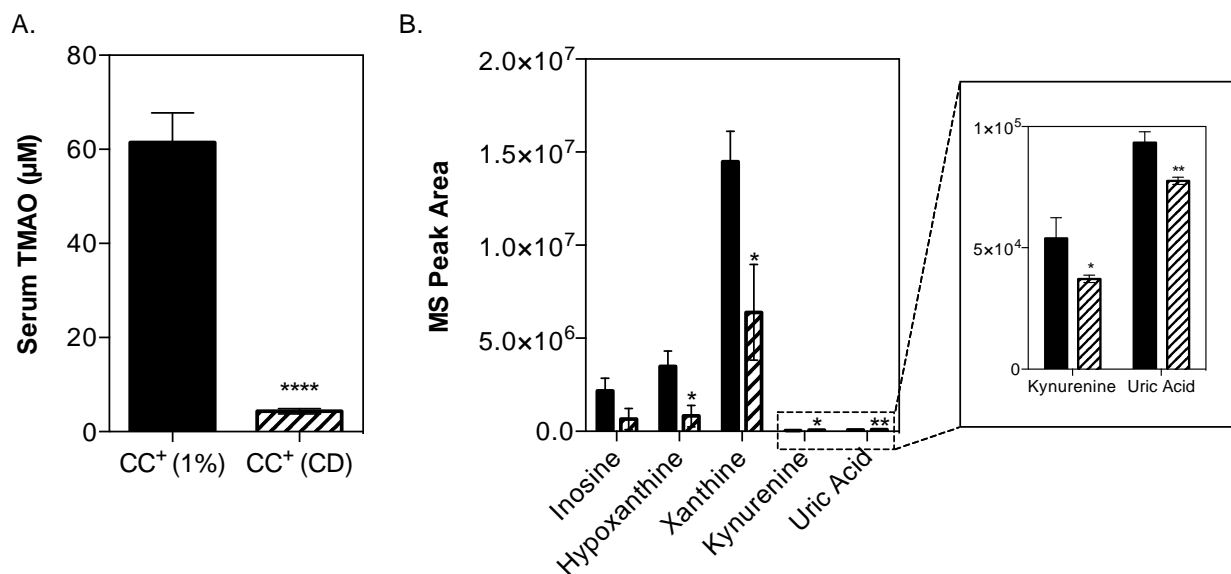


Fig. S2. Serum levels of metabolites related to purine metabolism detected in mice fed the choline-supplemented diet vs. choline-deficient diet. Related to Fig. 4. C57BL/6 females were colonized with the CC⁺ community and maintained for 2 weeks on either a 1% (wt/wt) choline-supplemented diet (black bars) or choline-deficient (CD) diet (striped bars). Mice were fasted for 4 h prior to sacrifice where serum was collected. **(A)** Serum TMAO (9-13 animals in each experimental group). **(B)** Purine metabolism. Serum metabolome analysis was conducted using uHPLC-MS/MS (5 animals in each experimental group). All values are averages \pm SEMs. Values that were significantly different (Student's t-test) are indicated: *, $P < 0.05$; **, $P < 0.01$, ****, $P < 0.0001$.

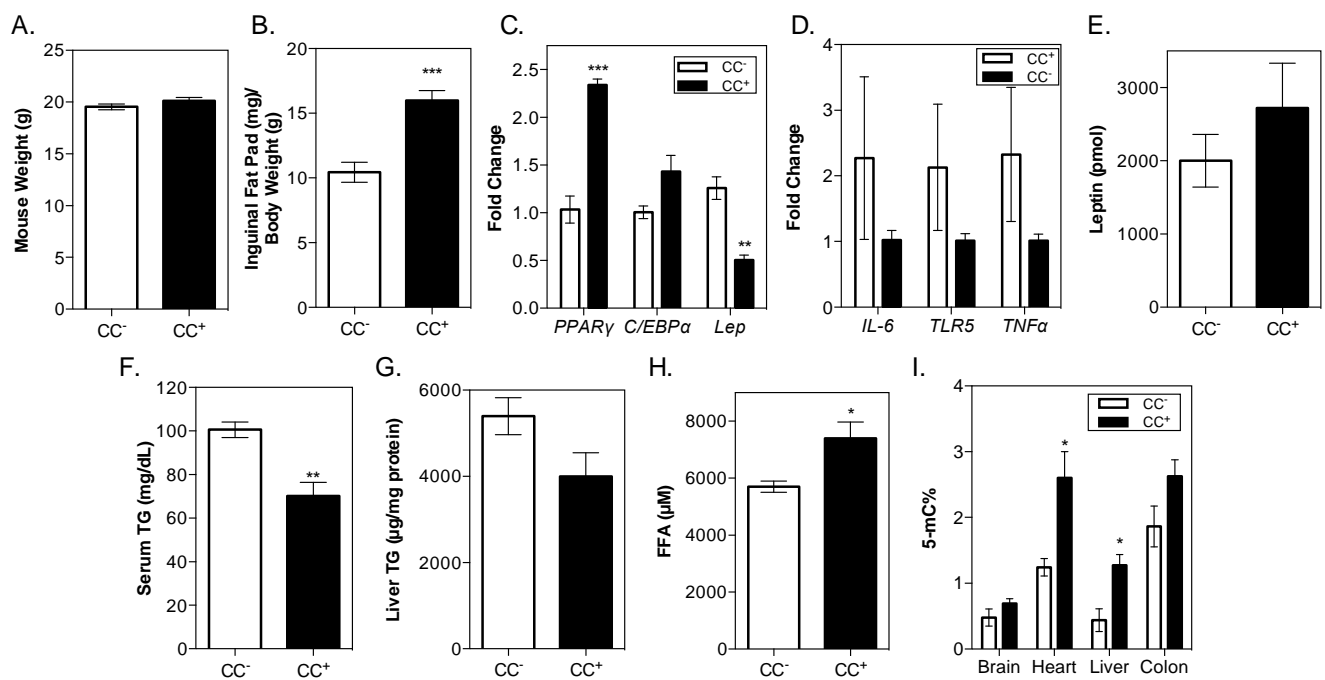


Fig. S3. Acute host responses to microbial choline metabolism. Related to Fig. 5 and Fig. 6. Phenotypic characterization of mice colonized with the CC⁺ and CC⁻ community maintained on a 1% choline diet for two weeks did not reveal changes in body weight between both groups of mice, however, animals colonized with the CC⁺ community showed significantly larger inguinal fat pads than mice colonized with the CC⁻ community (**A**, **B**). Adipogenesis is tightly regulated by a transcriptional cascade in which PPAR γ and members of the C/EBP family are key players (Siersbaek et al., 2010). qRT-PCR analysis for PPAR γ and C/EBP α on adipose tissue collected from both groups of mice (after 4 h of fasting) showed higher expression levels in mice colonized with the CC⁺ community (**C**). Expansion of adipose tissue is associated with increased production of several inflammatory cytokines and adipokines including IL-6, TNF α , and leptin (Ahima and Flier, 2000). Additionally, both humans and rodents with increased body mass exhibit elevated TLR5 expression (Pekkala et al., 2015). qRT-PCR analysis confirmed pro-inflammatory cytokines IL-6 and TNF α , along with TLR5, trended to be increased in the adipose of CC⁺ mice (**D**). TLR5 was up-regulated in the livers of the same mice (**Table S1**). We found that expression of *Lep* was significantly down-regulated in adipose tissue from mice colonized with the CC⁺ community (**C**). Increases in plasma levels of leptin reduce its own expression in adipose tissue through an autoregulatory feedback mechanism (Wang et al., 1999). In line with these reports, circulating leptin levels were increased in the CC⁺ mice compared to the CC⁻ (**E**). Leptin lowers lipid levels in tissues and plasma by stimulating fatty acid oxidation and impeding hepatic triglyceride (TG) secretion (rather than peripheral TG uptake) (Huang et al., 2006). Both hepatic and serum levels of TG were significantly reduced in mice colonized with the CC⁺ community (**F**, **G**). Moreover, RNAseq analyses of livers collected from these mice showed increased expression of genes associated with fatty acid oxidation in mice colonized with the CC⁺ community (**Table S1**). Consistent with this increase in fatty acid oxidation, higher circulating levels of free fatty acids (FFA) were observed (**H**). Changes in DNA methylation were also observed after only 2 weeks of colonization in multiple tissues (**I**). All values are averages \pm SEMs. Values that were significantly different (Student's t-test) are indicated: *, P < 0.05, **, P < 0.01, ***, P < 0.001.

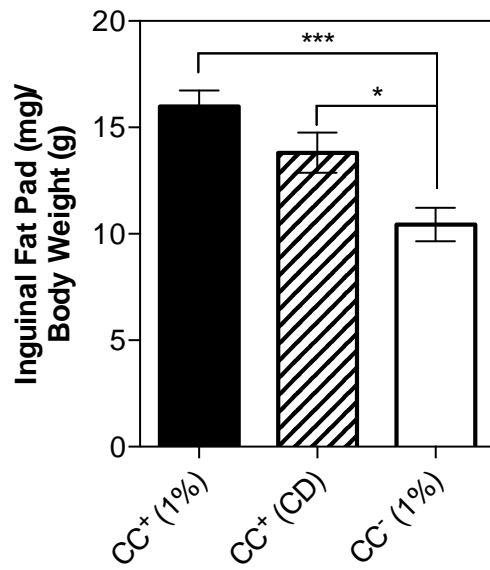


Fig. S4. Microbial choline metabolism increases adiposity. Related to Fig. 5 and Fig. S3. C57BL/6 females (8-13 animals in each experimental group) were colonized with the CC⁺ or CC⁻ community and maintained for 2 weeks on a 1% (wt/wt) choline diet or choline deficient diet (CD). Mice were fasted for 4 h prior to sacrifice. All values are averages \pm SEMs of inguinal fat pad mass normalized to body weight. Values that were significantly different (ANOVA) are indicated: *, $P < 0.05$, ***, $P < 0.001$.

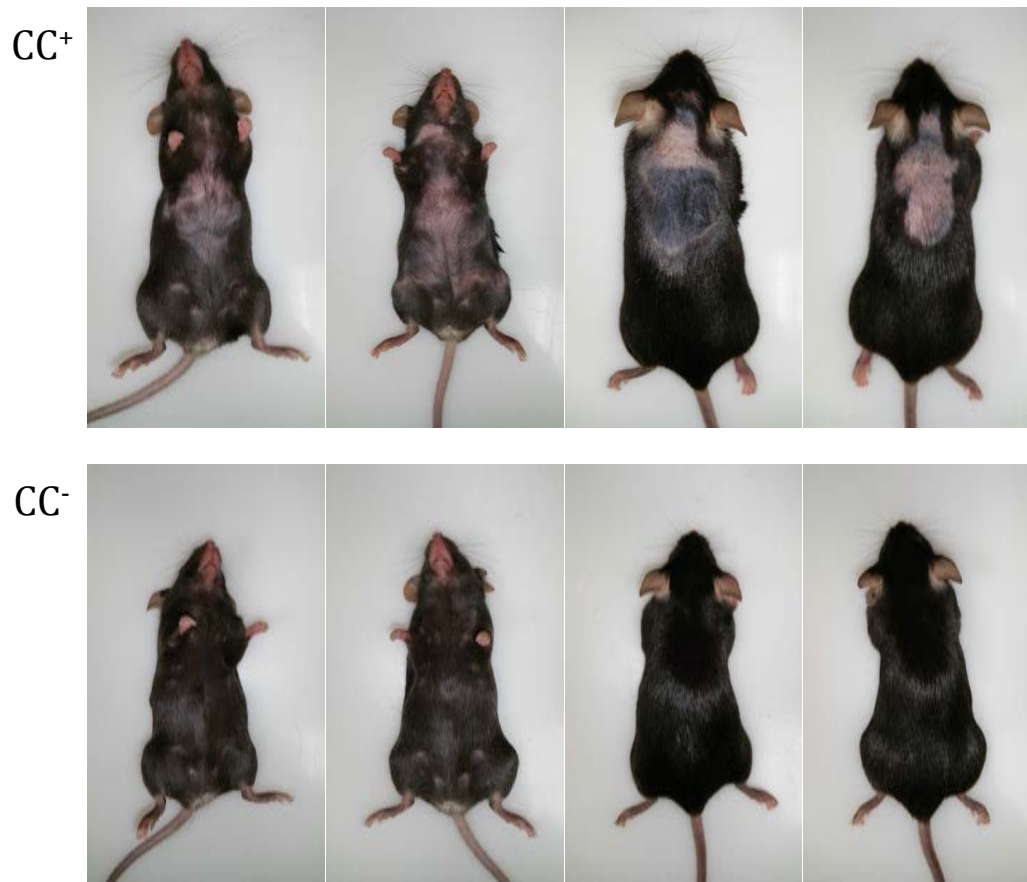


Fig. S5. Microbial choline utilization elicits F₀ barbering. Related to Fig 7. ApoE^{-/-} females were colonized with either the CC⁺ or CC⁻ community (8-10 animals per group) at 4 weeks of age and maintained for 14 weeks on a 1% (wt/wt) choline diet. Images were taken under isoflurane anesthesia. Each picture shows a different mouse and pictures are representative of each group.

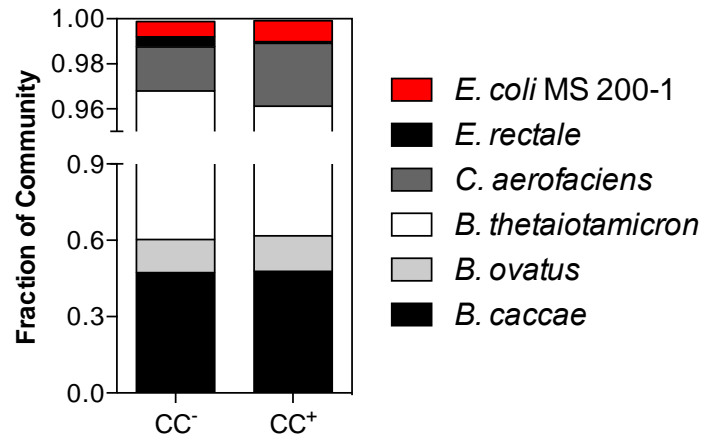


Fig. S6. F₁ community composition. Related to Fig 7. ApoE^{-/-} male and female mice were colonized with either the CC⁺ or CC⁻ community for 4 weeks and maintained on a 1% (wt/wt) choline diet. Mating trios were formed (2 per community) and females were allowed to carry pregnancy to term for two independent litters. Ceca from F₁ progeny were collected at time of sacrifice. Cecal community composition was determined by amplicon sequencing of the variable 4 (V4) region of the 16S rRNA gene using the Illumina MiSeq platform. All values are averages from 6 mice per community.

Table S1. Differentially expressed hepatic genes. Related to Fig. 3, Fig. 4, and Fig. S3.

Gene ID	PPDE ^a	Fold Change (CC ⁺ :CC ⁻)	Gene Association	Gene Annotation
<i>Fxn</i>	0.96	0.7	Apoptosis/ROS	Frataxin
<i>Fgd5</i>	0.95	0.7	Apoptosis	FYVE, RhoGEF and PH domain containing 5
<i>Dnase1l3</i>	1	0.71	Apoptosis	Deoxyribonuclease 1-like 3
<i>S100a10</i>	0.98	0.71	Thrombosis	S100 calcium binding protein A10 (calpactin)
<i>Eif3h</i>	1	0.73	Apoptosis	Eukaryotic translation initiation factor 3, subunit H
<i>Pigy</i>	1	0.74		Phosphatidylinositol glycan anchor biosynthesis, class Y
<i>Hspe1</i>	0.96	0.74	Apoptosis	Heat shock protein 1 (chaperonin 10)
<i>Ndufb2</i>	0.96	0.74	Apoptosis	NADH dehydrogenase (ubiquinone) 1 beta subcomplex, 2
<i>Ybx1</i>	1	0.76		Y box protein 1
<i>Fkbp1a</i>	1	0.76		FK506 binding protein 1a
<i>Ehd3</i>	0.96	0.76	Thrombosis	EH-domain containing 3
<i>S100a16</i>	1	0.77		S100 calcium binding protein A16
<i>Commd6</i>	0.97	0.77		COMM domain containing 6
<i>Fam134b</i>	1	0.79	Apoptosis	Family with sequence similarity 134, member B
<i>Arpc5l</i>	0.97	0.79		Actin related protein 2/3 complex, subunit 5-like
<i>Dnajc15</i>	1	0.8	ROS	DnaJ heat shock protein family (Hsp40) member C15
<i>Pfkfb2</i>	0.98	0.8		6-phosphofructo-2-kinase/fructose-2,6-biphosphatase 2
<i>2700060E02Rik</i>	1	0.81		RIKEN cDNA 2700060E02 gene
<i>Slc43a3</i>	1	0.81		Solute carrier family 43, member 3
<i>Mrpl13</i>	1	0.82		Mitochondrial ribosomal protein L13
<i>Ccdc107</i>	0.99	0.82		Coiled-coil domain containing 107
<i>Dnajc19</i>	0.91	0.82	Apoptosis	DnaJ heat shock protein family (Hsp40) member C19
<i>Tmem126a</i>	0.92	0.84		Transmembrane protein 126A
<i>Ghitm</i>	1	1.11		Growth hormone inducible transmembrane protein
<i>Pdlim5</i>	1	1.17		PDZ and LIM domain 5
<i>Zfyve26</i>	0.94	1.18		Zinc finger, FYVE domain containing 26
<i>Atl3</i>	0.99	1.19		Atlantin GTPase 3
<i>Trappc8</i>	1	1.2		Trafficking protein particle complex 8
<i>Acad8</i>	1	1.21		Acyl-Coenzyme A dehydrogenase family, member 8
<i>Sacm1l</i>	0.97	1.21		SAC1 (suppressor of actin mutations 1, homolog)-like
<i>Atp6v1a</i>	1	1.22	ROS	ATPase, H ⁺ transporting, lysosomal V1 subunit A
<i>Itgav</i>	1	1.27		Integrin alpha V
<i>Bdh1</i>	0.99	1.28		3-hydroxybutyrate dehydrogenase, type 1
<i>Hadhb</i>	1	1.31	Fatty Acid Oxidation	Hydroxyacyl-Coenzyme A dehydrogenase/3-ketoacyl-Coenzyme A thiolase/enoyl-Coenzyme A hydratase (trifunctional protein), beta subunit
<i>Glce</i>	1	1.32		Glucuronyl C5-epimerase
<i>Tmem184a</i>	0.91	1.32		Transmembrane protein 184a
<i>Mib1</i>	1	1.33		Mindbomb homolog 1
<i>Lonp2</i>	1	1.37	ROS/Fatty Acid Oxidation	Lon peptidase 2, peroxisomal
<i>Slc30a1</i>	1	1.37		Solute carrier family 30 (zinc transporter), member 1
<i>Shprh</i>	1	1.39		SNF2 histone linker PHD RING helicase
<i>Gna12</i>	1	1.41		Guanine nucleotide binding protein, alpha 12
<i>1300010F03Rik</i>	0.91	1.41		von Willebrand factor A domain containing 8
<i>Tgoln2</i>	1	1.42		Trans-golgi network protein 2
<i>Fut8</i>	0.99	1.42		Fucosyltransferase 8
<i>March6</i>	1	1.43		Membrane-associated ring finger (C3HC4) 6
<i>Lrp4</i>	1	1.5		Low density lipoprotein receptor-related protein 4
<i>Abcb4</i>	0.98	1.51		ATP-binding cassette, sub-family B (MDR/TAP), member 4
<i>Adra1a</i>	0.91	1.52	Apoptosis	Adrenergic receptor, alpha 1a
<i>Retsat</i>	0.97	1.61		Retinol saturase (all trans retinol 13,14 reductase)
<i>Ptpn4</i>	1	1.65		Protein tyrosine phosphatase, non-receptor type 4
<i>Slc4a4</i>	1	1.75		Solute carrier family 4 (anion exchanger), member 4
<i>Syt14</i>	0.92	1.79	Thrombosis	Synaptotagmin-like 4
<i>Tlr5</i>	1	1.92	Apoptosis	Toll-like receptor 5
<i>Tgtp2</i>	1	2.53		T cell specific GTPase 2

^aPPDE- posterior probability of being differentially expressed

Table S2. Key Resource Table supplemental oligonucleotides. Related to Key Resource Table.		
REAGENT or RESOURCE	SOURCE	IDENTIFIER
Deletion of <i>cutC</i> forward primer: TGGAGCGGCAATATCGCTCAATGCCACTGATAACAAGAACTGGAGACCCTGTGT AGGCTGGAGCTGCTTC	IDT	N/A
Deletion of <i>cutC</i> reverse primer: TCCGGTTGCGATCCGTTTTATCAGAACTTCTCAATCACCGTACGGCTGATCATATG AATATCCTCCTTAG	IDT	N/A
Deletion of <i>cutD</i> forward primer: GACATTTTCAGGAGGCAAGCGTGAGCGCAAATAAAGAATTAAGCGGACGAGTGT AGGCTGGAGCTGCTTC	IDT	N/A
Deletion of <i>cutD</i> reverse primer: ACTGTTCAATTTACGGCTCCTTAATGACGAACTAAGCGAATATCAAAATCCATAT GAATATCCTCCTTAG	IDT	N/A
Complementation of $\Delta cutC$ forward primer: CCGGAATTCTCGCCAGGCCTGGAGCGGCA	IDT	N/A
Complementation of $\Delta cutC$ reverse primer: CTAGTCTAGATCAGAACTTCTCAATCACCG	IDT	N/A
Complementation of $\Delta cutD$ forward primer: CCGGAATTCTAAGACGGATCGCAACCGGA	IDT	N/A
Complementation of $\Delta cutD$ reverse primer: CTAGTCTAGATTAATGACGAACTAAGCGAA	IDT	N/A
<i>Actb</i> qRT-PCR forward primer: CTACAGCTTACCACCACAG	IDT	N/A
<i>Actb</i> qRT-PCR reverse primer: GCAGCTCATAGCTCTTCTCC	IDT	N/A
<i>C/EBPα</i> qRT-PCR forward primer: GCACCTCCACCTACATCC	IDT	N/A
<i>C/EBPα</i> qRT-PCR reverse primer: ATGGCTAACTCACAACCTCAG	IDT	N/A
<i>IL-6</i> qRT-PCR forward primer: CCACTTCACAAGTCGGAGGCTTA	IDT	N/A
<i>IL-6</i> qRT-PCR reverse primer: GCAAGTGCATCATCGTTGTTTCATAC	IDT	N/A
<i>Lep</i> qRT-PCR forward primer: CCTGTGGCTTTGGTCCTATC	IDT	N/A
<i>Lep</i> qRT-PCR reverse primer: ATACCGACTGCGTGTGTGAA	IDT	N/A
<i>PPARγ</i> qRT-PCR forward primer: CCACAGTTGATTTCTCCAGCATTTC	IDT	N/A
<i>PPARγ</i> qRT-PCR reverse primer: CAGGTTCTACTTTGATCGCACTTTG	IDT	N/A
<i>TLR5</i> qRT-PCR forward primer: GGACACTGAAGGATTTGAAGATG	IDT	N/A
<i>TLR5</i> qRT-PCR reverse primer: GGACCATCTGTATGCTTGGAATA	IDT	N/A
<i>TNFα</i> qRT-PCR forward primer: ATGAGCACAGAAAGCATGATC	IDT	N/A
<i>TNFα</i> qRT-PCR reverse primer: TACAGGCTTGTCACTCGAATT	IDT	N/A
Mouse sexing forward primer: GATGATTTGAGTGGAATGTGAGGTA	McFarlane et al., 2013	N/A
Mouse sexing reverse primer: CTTATGTTTATAGGCATGCACCATGTA	McFarlane et al., 2013	N/A